Calculation of ir band profiles of diatomic molecules dissolved in liquids[a)]

B. C. Sanctuary

Department of Chemistry, McGill University, 801 Sherbrooke Street, West Montreal, Canada H3A 2K6

Dominique Richon

Ecole Nationale Supérieure des Mines, Boulevard Saint-Michel 60 (VI), Paris, France
(Received 13 February 1978)

Using a memory function approach, ir band profiles are calculated for diatomic molecules dissolved in a solvent of orientable molecules. The motivation is to extract the solvent correlation function from the solute spectrum. The approach is tested by fitting the theory to experimental data for CO and DCl. The agreement is encouraging, indicating that theory should provide a basis for testing models for liquid dynamics.

Recently,[1] infrared spectroscopy has been used as a tool to probe the local orientational anisotropies of liquid chainlike molecules (e.g., the alkanes). The technique involves dissolving a probe molecule (e.g., CO or DCl) in an alkane solvent and the ir spectrum of the probe molecule studied as a function of alkane chain length and degree of branching. It is observed that these properties of the solvent lead to varying degrees of broadening of the solute (probe) spectra. Moreover, since the correlation time obtained from the ir band shape is a linear function of the ratio of the Q branch maximum to the R branch maximum, the Q/R ratio is used as a measure of solvent effect. A variety of trends has been reported using this parameter.[1]

It is clear that the local anisotropic properties of the alkanes lead to a force field about the probe molecule which varies with the solvent. Hence, studies of the probe molecule's spectra should reveal information about the local forces at play in the solvent. The purpose of this paper is to present some preliminary results in which the memory function approach of describing liquids[2] is employed to extract information about the solvent interactions from the solute ir spectra. Since the emphasis at this stage is to describe the solute spectra, calculations of the solvent dynamics are not undertaken. In particular, the relevant parameters which are required to describe the solvent interactions are left as empirical parameters for the time being.

The main difference between the approach described here and other studies of ir spectra[3] is that the *active molecule is not of fundamental importance*. Rather, the perturbations due to the solvent which lead to varying degrees of broadening of the solute spectra are of interest. Therefore, the initial aim is to extract the *solvent* correlation function from the ir spectrum, and not the solute correction function. A projection operator theory[4] is well suited for this and is described in the following.

It is assumed that the probe molecule is present at sufficiently low concentrations so that solute–solute interactions are negligible. Moreover, since the broadening of the solute spectrum arises from anisotropic solvent–solute interactions, it is assumed that the solvent-solute forces are weaker than the solvent-solvent forces. This division provides a basis for separating the solvent and solute observables, retaining only a relatively weak interaction between the two. The problem is essentially that of pressure broadening of the solute molecule and Fano's theory[5] can be employed.

Denoting the Liouville operators for the solvent, the solute, and for the solvent–solute interactions by, respectively, $\mathcal{L}_S$, $\mathcal{L}_s$, and $\mathcal{V}$, the normalized spectral density for the solute can be written

$$\hat{I}(\omega) = \frac{1}{\pi}\,\mathrm{Re}\int_0^\infty e^{i\omega t}\langle\hat{\mu}\cdot\hat{\mu}(t)\rangle\,dt \tag{1}$$

$$= -\frac{1}{\pi}\,\mathrm{Im}\,\mathrm{Tr}_s(\rho_{0s}^{1/2}\mu)^\dagger(\omega-\omega_0-\mathcal{L}_s-\langle M_c(\omega)\rangle_S)^{-1}(\rho_{0s}^{1/2}\mu),$$

where μ is the dipole moment operator of the solute ($\mu = \mu\hat{\mu}$)

$$\mu(t) \equiv e^{i(\mathcal{L}_S+\mathcal{L}_s+\mathcal{V})t}\,\mu\ , \tag{2}$$

and

$$I(\omega) = \left(\frac{8\pi^2 n\omega^2\mu^2}{3kT}\right)\hat{I}(\omega)\ , \tag{3}$$

with n being the solute concentration. The trace is over all solute variables, ω_0 is the vibrational frequency, and the equilibrium density operator for the solvent and solute is assumed to be factorizable into solute, solvent parts,

$$\rho_0 = \rho_{0s}\rho_{0S}\ . \tag{4}$$

The quantity of most interest is the $M_c(\omega)$ operator which is averaged over solvent variables and is given by

$$\langle M_c(\omega)\rangle_S = \langle\mathcal{V}\rangle_S - i\lim_{\epsilon\to 0}\int_0^\infty \langle\mathcal{V}e^{-i\mathcal{L}_S t}\mathcal{V}\rangle_S\, e^{i(\omega+i\epsilon)t}\,dt\ . \tag{5}$$

In obtaining the above expressions, it is assumed that the solute dipole correlation function is a product of the rotational and vibrational correlation functions. The latter relaxes much more slowly than the former[1,3,6] and is taken as a constant. Also, consistent with the weak solvent–solute anisotropic interactions, it is assumed that only pure solvent dynamics govern the time correlation function $\langle\mathcal{V}\mathcal{V}(t)\rangle_s$, so $\mathcal{V}(t) = \exp(-i\mathcal{L}_s t)\mathcal{V}$.

Equation (5) contains two main contributions. The first term accounts for differences of energy between

a)Work supported by the National Research Council Canada and the Ministère de l'Education du Province de Québec.

 0021-9606/78/6908-3782$01.00

the upper and lower solute states as a result of the solvent–solute interactions. As such, it is a frequency shift. The second is the Fourier transform of a correlation function and leads to broadening (real part) and shifting (imaginary part). However, both terms are still operators in the solute variables. These can only be separated by specifying $\mathcal{U}$ more explicitly.

The anisotropic part of the solvent–solute forces V_1 is assumed to be of the form

$$V_1 = (4\pi)^{3/2} \sum_{M=-1}^{1} Y^*_{1M}(\hat{r}_s) C_{1M}(\mathbf{R}, \hat{r}_S) , \tag{6}$$

where $Y_{1M}(\hat{r}_s)$ describes the orientation of the probe molecule. $C_{1M}(\mathbf{R}, \hat{r}_S)$ depends upon the local orientation of the solvent molecule and the solvent–solute separation $\mathbf{R}$. The quantity $C_{1M}(\mathbf{R}, \hat{r}_S)$ should not be inferred to be due to a dipole moment of the solvent alone. Rather, all orders of the anisotropy of the solvent are coupled to a first rank tensor having a form such as

$$C_{1M}(\mathbf{R}, \hat{r}_S) = \sum_{\substack{LL' \\ NN'}} b_L(R) Y_{LN}(\hat{R})\, Y_{L'N'}(\hat{r}_S) \begin{pmatrix} L & L' & 1 \\ N & N' & M \end{pmatrix} . \tag{7}$$

Substitution of this form for V_1 into Eq. (5) and tracing over all solute states gives (note $\mathcal{U}A = [V_1, A]_-$).

$$\hat{I}(\omega) = -\pi^{-1}\,\mathrm{Im} \sum_{\substack{J\bar{J} \\ J'\bar{J}'}} (p_J/2J+1)^{1/2}\, d_{JJ'} (\mathbf{R}^{-1})_{JJ'\bar{J}\bar{J}'} (p_J/2\bar{J}+1)^{1/2} d_{\bar{J}\bar{J}'} , \tag{8}$$

where p_J are the Boltzmann weights for the Jth solute rotational state, $d_{JJ'} = d_{J'J} = \sqrt{J+1}\,\delta_{J',J+1}$, and $\mathbf{R}$ is a relaxation matrix, one element of which is

$$R_{JJ'\bar{J}\bar{J}'} = [(\omega - \omega_0 - \omega_{JJ'})\delta_{J\bar{J}}\delta_{J'\bar{J}'} - \langle M_c(\omega)\rangle_{JJ'\bar{J}\bar{J}'}] . \tag{9}$$

The $\langle M_c(\omega)\rangle_{JJ'\bar{J}\bar{J}'}$ consists of J dependent kinematic factors arising from the trace over solute internal states and dynamical factors arising from pure solvent effects. it is given by

$$\langle M_c(\omega)\rangle_{JJ'\bar{J}\bar{J}'} = \Delta_{JJ'}\delta_{J\bar{J}}\delta_{\bar{J}'J'} + \frac{3i}{2\pi}\left\{\delta_{J\bar{J}}\delta_{\bar{J}'J'} - (-1)^{J+\bar{J}} \begin{Bmatrix} J & 1 & J' \\ J' & 1 & \bar{J} \end{Bmatrix} [(2J+1)(2\bar{J}+1)(2\bar{J}'+1)(2J'+1)]^{1/2} \times \begin{pmatrix} J & 1 & \bar{J} \\ 0 & 0 & 0 \end{pmatrix} \begin{pmatrix} \bar{J}' & 1 & J' \\ 0 & 0 & 0 \end{pmatrix} \right\} [\gamma(\omega) + i\delta(\omega)] , \tag{10}$$

which is in terms of $3-j$ and $6-j$ coefficients and where the solvent dynamics are contained in the terms

$$\gamma(\omega) + i\delta(\omega) = \frac{1}{3}\int_0^\infty e^{i\omega t} \langle C_1 \cdot C_1(t)\rangle_S\, dt . \tag{11}$$

The solvent correlation function may be evaluated by the application of some model.[7–10] These approaches usually take the form of an exponential decay. Assuming this to be the case, the width is given by

$$\gamma(\omega) = \langle C_1^2\rangle_S \frac{\tau_S}{1+\omega^2\tau_S^2} \tag{12}$$

and the shift by

$$\delta(\omega) = \langle C_1^2\rangle_S \frac{\omega\tau_S^2}{1+\omega^2\tau_S^2} , \tag{13}$$

where τ_S is the solvent correlation time. Another source of frequency shifting arises from the first term in Eq. (5). This is written as

$$\Delta_{JJ'} = \Delta_{01} + \Delta^0_{JJ'} , \tag{14}$$

where Δ_{01} accounts for the vibrational spacing shift while $\Delta^0_{JJ'}$ accounts for the rotational level shift.

The quantities $\gamma(\omega)$, $\delta(\omega)$, and $\Delta_{JJ'}$ require detailed knowledge of the solvent–solvent interactions for their evaluation. In the following, these, or equivalently $\langle C_1^2\rangle$, τ_S, and $\Delta_{JJ'}$, are treated as empirical parameters to test the validity of the form of Eq. (8) to reproduce the experimental data.

RESULTS

Study of the band profile was undertaken by retaining only resonant off-diagonal terms in the relaxation matrix [i.e., $\langle M_c(\omega)\rangle_{JJ\pm1,J\pm1,J} \neq 0$]. This means that collisional J changes in the P and R branches of $J \rightarrow J+1$ and $J+1 \rightarrow J$ are included as well as reorientation. What is neglected by the resonance collisional approximation are those collisional terms $J \rightarrow J \pm 1$ and $J \pm 1 \rightarrow J \pm 2$ [i.e., $\langle M_c(\omega)\rangle_{J,J\pm1,J\pm1,J\pm2} \cong 0$]. Inclusion of these latter terms makes only a small change to the shape of the band profile in the cases studied since the nonzero collisional frequencies which arise have the effect of reducing (phase randomizing) those off-diagonal terms in the relaxation matrix. With this assumption, the full relaxation matrix uncouples to give a sum of 2×2 matrices so that

$$I(\omega) = \frac{8\pi n\,\omega^2\mu^2}{3kT}\,\mathrm{Im}\sum_J \frac{p_J}{D_J}\left[\frac{(J+1)^2}{(2J+1)(2J+3)}\right]^{1/2}\left(\left\{\omega - \omega_0 + \omega_{J,J+1} + \Delta_{J,J+1} + \frac{i3}{2\pi}(\gamma+i\delta)\right\} + \left\{\frac{3}{2\pi}\left[\frac{p_{J+1}}{P_J}\frac{J(J+2)}{(2J+3)^2}\right]^{1/2}(\gamma+i\delta)\right\} + \left\{\left[\frac{p_{J+1}}{p_J}\frac{(2J+1)}{(2J+3)}\right](\omega - \omega_0 - \omega_{J,J+1} - \Delta_{J,J+1} + i\frac{3}{2\pi}(\gamma+i\delta))\right\}\right) , \tag{15}$$

where

$$D_J\left\{\left[\omega - \omega_0 + \frac{i3}{2\pi}(\gamma+i\delta)\right]^2 - (\omega_{J,J+1} + \Delta_{J,J+1})^2 + \frac{9}{16\pi^2}\left[\frac{J(J+2)}{(2J+1)(2J+3)}\right](\gamma+i\delta)^2\right\} . \tag{16}$$

TABLE I. Values of parameters used to calculate the band profiles.

	τ_s(sec)	$\langle C_1^2\rangle\tau_S$ (cm^{-1})	Δ_0 (cm^{-1})	Δ_1 (cm^{-1})
DCl	3.96×10^{-15}	150	30	1.0
CO	3.96×10^{-15}	150	15	0.15

Various values for $\langle C_1^2\rangle$, τ_s, and $\Delta^0_{JJ'}$ were chosen. Since Δ_{01} merely shifts the whole profile, it was absorbed into ω_0. Several features emerged.

Firstly, the dependence of $\gamma(\omega)$ and $\delta(\omega)$ on ω could not be distinguished. This was because a decrease in the Lorentzian parts of Eqs. (12) and (13) by increasing $\omega\tau_S$ could be compensated by increasing $\langle C_1^2\rangle$. The relevant solute line width parameter is $\langle C_1^2\rangle\tau_S$. Hence τ_S is chosen to be small. It is worthwhile to note, however, that a width with a frequency dependence of $\tau(1+\omega^2\tau^2)^{-1}$ was suggested empirically by Gordon,[9] and follows quite naturally from the treatment here.

Secondly, it was impossible to obtain the observed Q branch without including the frequency shift $\Delta^0_{JJ'} = -\Delta^0_{J'J}$. Moreover, it was necessary for a reasonable fit to the data to have $\Delta^0_{JJ'}$ decrease with increasing JJ'. This is conjectured to result from the increased gyroscopic stability of the solute molecule with increasing J. A form which seemed adequate is[11]

$$\Delta^0_{J+1,J} = \Delta_0 - J(J+1)\Delta_1 , \tag{17}$$

with the requirement that $\Delta^0_{J+1,J} > 0$ for all J. This has the effect of shifting P and R lines closer together.

Combining the above observations and choosing the values in Table I, the band profiles were calculated. These are shown in Fig. 1 along with the experimental curves for DCl and CO dissolved in bicyclopentyl.[6] Since n, μ, and T are constants in Eq. (15), the plotted curves retains (const.)$\omega^2 I(\omega)$. The only difference between the CO and DCl profile calculations comes from changing ω_0, the rotational constant, and Δ_1, Δ_0. The frequency shift ratio is seen from Table I to be 2:1 for DCl:CO, which is approximately the ratio of the rotational constants.

The solvent dynamical effects should be the same for both solute molecules. Hence, it is reasonable that τ_S and $\langle C_1^2\rangle\tau_S$ be equal for both the DCl and CO spectra when the same solvent is used.

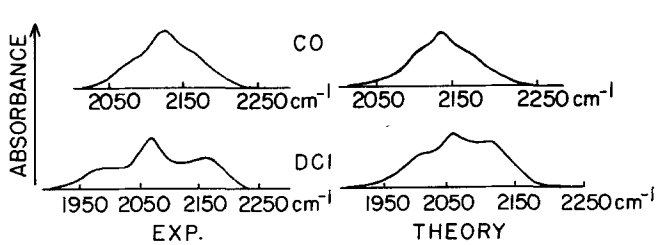

FIG. 1. Experimental and theoretical infrared spectra of DCl and CO dissolved in bicyclopentyl.

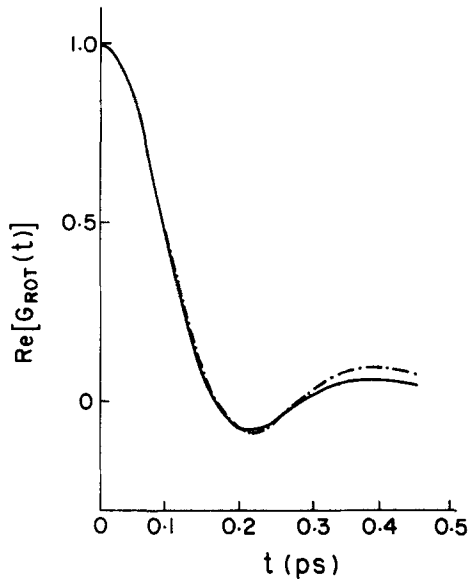

FIG. 2. Solute correlation function calculated from the infrared spectrum of DCl dissolved in 3, 3-diethylpentane (-·-) along with the theoretical curve (—).

Figure 2 shows the solute correlation function, calculated from a band profile obtained with $\tau_S = 3.96\times10^{-15}$ sec, $\tau_S\langle C_1^2\rangle = 100$ cm^{-1}, $\Delta_1 = 30$ cm^{-1}, and $\Delta_2 = 1.00$ cm^{-1}. The dashed curve is the experimentally obtained correlation function obtained by Fourier transforming the band profile for DCl dissolved in 3, 3-diethylpentane.[6]

The results in Figs. 1 and 2 are typical and it is possible to obtain reasonable fits to a variety of experimental results for CO and DCl dissolved in different alkanes. As an illustration of the variety of curves obtained, Figs. 3–6 show the resulting band profiles and correlation functions as the parameters are varied. Figures 3 and 5 show the results for, respectively, DCl and CO with no frequency shift. The curves move from a gaslike spectrum (free rotor limit) to a single peak (Debye line shape limit). Introduction of frequency

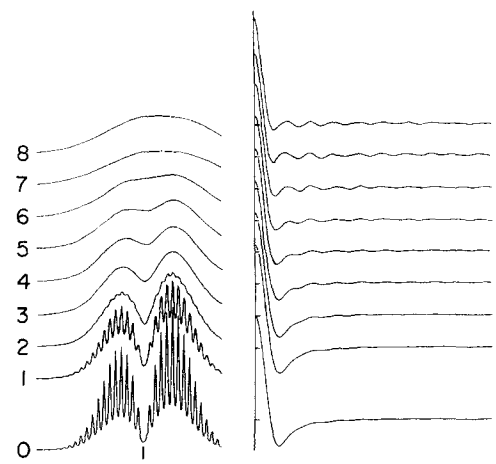

FIG. 3. Calculated ir spectra and correlation functions for DCl with the values in Table II.

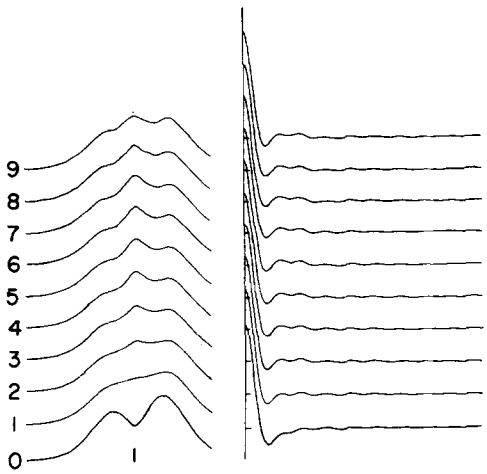

FIG. 4. Calculated ir spectra and correlation functions for DCl with values in Table II.

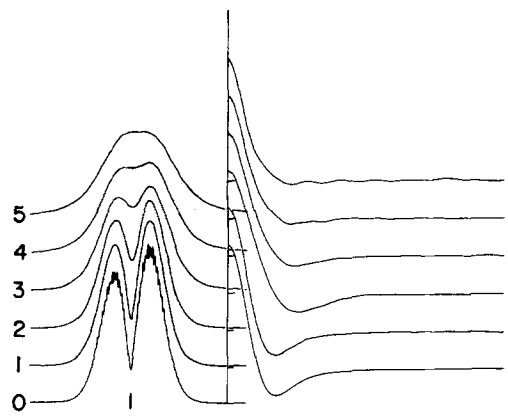

FIG. 5. Calculated ir spectra and correlation functions for CO with values in Table II.

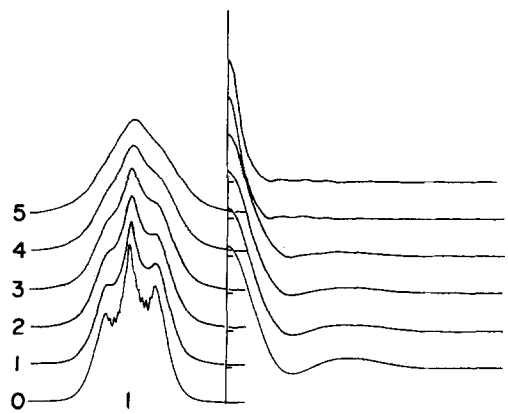

FIG. 6. Calculated ir spectra and correlation functions for CO with values in Table II.

TABLE II. Values used to calculate the band profiles from Eq. (15).

Spectra		τ_S (cm)	$\langle C^2\rangle\tau_S$ (cm^{-1})	Δ_1 (cm^{-1})	Δ_2 (cm^{-1})
Fig. 3	0	1.19×10^{-4}	15.0	0.0	0.0
	1	1.19×10^{-4}	25.0	0.0	0.0
	2	1.19×10^{-4}	50.0	0.0	0.0
	3	1.19×10^{-4}	100.0	0.0	0.0
	4	1.19×10^{-4}	150.0	0.0	0.0
	5	1.19×10^{-4}	200.0	0.0	0.0
	6	1.19×10^{-4}	300.0	0.0	0.0
	7	1.19×10^{-4}	400.0	0.0	0.0
	8	1.19×10^{-4}	500.0	0.0	0.0
Fig. 4	0	1.19×10^{-4}	150.0	5.0	0.17
	1	1.19×10^{-4}	150.0	10.0	0.33
	2	1.19×10^{-4}	150.0	15.0	0.50
	3	1.19×10^{-4}	150.0	20.0	0.67
	4	1.19×10^{-4}	150.0	25.0	0.83
	5	1.19×10^{-4}	150.0	30.0	1.00
	6	1.19×10^{-4}	150.0	35.0	1.20
	7	1.19×10^{-4}	150.0	42.9	1.43
	8	1.19×10^{-4}	150.0	53.6	1.79
	9	1.19×10^{-4}	150.0	64.3	2.14
Fig. 5	0	1.19×10^{-4}	25.0	0.0	0.0
	1	1.19×10^{-4}	50.0	0.0	0.0
	2	1.19×10^{-4}	75.0	0.0	0.0
	3	1.19×10^{-4}	100.0	0.0	0.0
	4	1.19×10^{-4}	150.0	0.0	0.0
	5	1.19×10^{-4}	200.0	0.0	0.0
Fig. 6	0	1.19×10^{-4}	25.0	15.0	0.15
	1	1.19×10^{-4}	50.0	15.0	0.15
	2	1.19×10^{-4}	75.0	15.0	0.15
	3	1.19×10^{-4}	100.0	15.0	0.15
	4	1.19×10^{-4}	150.0	15.0	0.15
	5	1.19×10^{-4}	200.0	15.0	0.15

shifts in Figs. 4 and 6 result in a "Q branch". The values used to calculate these curves from Eq. (15) are given in Table II. In Figs. 3–6, the mark on the frequency spectra indicates ω_0 while the tick on the correlation function axis indicates the zero value.

Clearly, by changing the parameters, it is possible to fit a wide range of data. However, based upon the present treatment, there is no *a priori* reason for knowing how the parameter should change with different solvents. Rather, the solvent correlation function $\langle C_1 \cdot C_1(t)\rangle_S$ requires evaluation based upon a viable model for molecular motions of chainlike molecules. The approach presented here shows that it is possible to extract a solvent correlation function from a probe molecule's ir spectrum. Hence, this treatment forms a phenomenological basis from which dynamical models can be tested and, hopefully, from which information about the local orientation of the liquids can be studied.

[1]D. Richon, D. Patterson, and G. Turrell, Chem. Phys. Lett. **36**, 492 (1975); Chem. Phys. **24**, 227 (1977); D. Richon and D. Patterson, Chem. Phys. Lett. **46**, 582 (1977); Chem. Phys. **24**, 335 (1977).

[2]See, for example, B. J. Berne and G. D. Harp, Adv. Chem. Phys. **17**, 63 (1970).

[3]See, for example, S. Bratoz, J. Rios, and Y. Guissani, J. Chem. Phys. **52**, 439 (1970); R. G. Gordon, J. Chem. Phys.

43, 1307 (1965).
[4]R. Zwanzig, *Lectures in Theoretical Physics*, edited by W. E. Brittin, B. W. Downs, and J. Downs (Interscience, New York, 1960), Vol. III, p. 106.
[5]U. Fano, Phys. Rev. **131**, 259 (1963).
[6]Dominique Richon, Ph. D. Thesis, McGill University, 1977.
[7]See, for example, D. Chandler, J. Chem. Phys. **60**, 3500 (1974); **60**, 3508 (1974).
[8]See, for example, M. L. Koszykowski and R. A. Marcus, J. Chem. Phys. **68**, 1216 (1978).
[9]R. G. Gordon, J. Chem. Phys. **44**, 1830 (1966).
[10]G. R. Alms, D. R. Bauer, J. I. Brauman, and R. Pecora, J. Chem. Phys. **59**, 5310 (1973).
[11]Recent work supports the symmetry and J trend of $\Delta_{J+1,J}$ based upon collisional perturbation of the rotational levels. The functional form in Eq. (17) is empirical.